Optics Letters

Mode-evolution-based coupler for high saturation power Ge-on-Si photodetectors

Matthew J. Byrd,[1,*] Erman Timurdogan,[1] Zhan Su,[1] Christopher V. Poulton,[1] Nicholas M. Fahrenkopf,[2] Gerald Leake,[2] Douglas D. Coolbaugh,[2] and Michael R. Watts[1]

[1]Research Laboratory of Electronics, Massachusetts Institute of Technology, 77 Massachusetts Avenue, Cambridge, Massachusetts 02139, USA
[2]College of Nanoscale Science and Engineering, State University of New York Polytechnic Institute, 257 Fuller Road, Albany, New York 12203, USA
*Corresponding author: mbyrd@mit.edu

Received 20 December 2016; accepted 23 January 2017; posted 30 January 2017 (Doc. ID 283098); published 14 February 2017

We propose a mode-evolution-based coupler for high saturation power germanium-on-silicon photodetectors. This coupler uniformly illuminates the intrinsic germanium region of the detector, decreasing saturation effects, such as carrier screening, observed at high input powers. We demonstrate 70% more photocurrent generation (9.1–15.5 mA) and more than 40 times higher opto-electrical bandwidth (0.7–31 GHz) than conventional butt-coupled detectors under high-power illumination. The high-power and high-speed performance of the device, combined with the compactness of the coupling method, will enable new applications for integrated silicon photonics systems.

OCIS codes: (230.5160) Photodetectors; (230.0250) Optoelectronics; (130.3120) Integrated optics devices.

https://doi.org/10.1364/OL.42.000851

Light detection is essential for wave-guided integrated electronic-photonic systems. Various techniques have been investigated for this purpose, such as bonding III–V photodetectors to a silicon wafer [1,2]. In contrast to bonding, the successful growth of germanium on a silicon wafer [3,4] has shown that germanium-on-silicon (Ge-on-Si) photodetectors are a viable option for near-infrared detection on a complementary metal-oxide-semiconductor (CMOS) compatible platform. Such devices have been studied extensively, with efforts focused on improving the performance of butt-coupled Ge-on-Si detectors [5–14]. Two major drawbacks to this coupling method are the large impedance mismatch between the silicon bus waveguide and the Ge-on-Si structure [7] and the strong absorption of incident light in the first few micrometers of the detector [1]. Both problems can lead to saturation in DC [15,16] and compression in RF [16–18] current generation under high-power illumination. To improve the saturation level, the peak intensity of the carriers within the detectors can be minimized by utilizing uni-traveling carrier designs in indium phosphide, which are bonded to a silicon/silicon-on-insulator (SOI) wafer requiring complex fabrication and design processes [1,2]. Another approach involves segmented designs based on tree networks of detectors with traveling-wave electrodes [19], increasing the dark current and lowering the sensitivity. Both approaches reduce high-power saturation effects but add complexity to the system.

Another solution is to re-engineer the coupler to more effectively illuminate the germanium region of a single waveguide-coupled photodetector. This can be done using mode evolution to transfer light from the silicon bus waveguide into the detector gradually and efficiently. Such a design is advantageous because it eliminates the modal interference that causes the locations of strong absorption seen in [1] and instead uniformly illuminates the detector. Furthermore, mode-evolution-based structures are inherently broadband and require less accuracy and precision in the fabrication process, making them more suitable to wafer-scale integrated photonics systems [20,21].

In this Letter, we demonstrate a compact and efficient mode-evolution-based coupler to transfer TE-polarized light from a silicon bus waveguide to a Ge-on-Si photodetector. Designed within a CMOS-compatible process, this coupler transfers input power from the bus waveguide into a few similar modes in the Ge-on-Si structure. Compared to a similar butt-coupled photodetector, the mode-evolution-based coupled detector generates 70% more DC photocurrent (15.5 versus 9.1 mA) at a high incident power of 28 mW. Furthermore, at a total input power of 4 mW, the mode-evolution-based coupled detector maintains a high opto-electrical bandwidth of 31 GHz compared to only 0.7 GHz in the butt-coupled detector.

The germanium detectors presented in [5–14] rely on some variation of butt coupling, which is defined here as having a silicon bus waveguide directly incident on the Ge-on-Si structure. By using this coupling method, all of the light in the bus waveguide is transferred into the photodetector at the waveguide-detector interface, causing two problems. First, butt-coupling excites modes in the detector with vastly different propagation constants so strong modal interference with high peak intensities can be observed. Second, all of the light is transferred into the germanium at once, so most of the absorption occurs in the first few micrometers of the detector [1]. Together, these two issues will produce discrete locations of high power density in the germanium, leading to saturation effects. One such effect is that trap sites on the germanium-silicon interface are occupied for longer fractions of time due to a high generation rate of free carriers. This decreases

the recombination rate of minority carriers and lowers the responsivity at high input powers [15]. Additionally, a large electron-hole pair density in a single location creates a large gradient of charge, inducing a strong electric field opposing the applied bias. This effect, called carrier screening, reduces the bandwidth at high powers because the carriers are not efficiently swept out of the detector [18].

To overcome these challenges, we propose a novel coupling method using mode evolution to transfer power into the Ge-on-Si region gradually and efficiently; this mode-evolution-based coupler is illustrated in Fig. 1(a). The coupler consists of two sections: a bend in the bus waveguide to bring it near the detector, gradually minimizing the impedance mismatch in order to not excite unwanted hybrid or back-propagating modes, and a linear asymmetric taper of the bus waveguide to transfer the input power from the bus to the Ge-on-Si structure. Importantly, this type of coupler is universal, allowing it to be attached to any stand-alone detector. Figure 1(b) shows the evolution and power transfer from the fundamental TE mode in the bus waveguide to the TE_{13} mode of the detector. In this simulation, the germanium width was narrowed to limit the number of guided modes and to match the index of the fundamental mode in the bus to the TE_{13} mode in the detector, suppressing coupling to unwanted modes. Cross-sectional views of the mode profile and device structure are shown in Fig. 1(c).

The key parameters in the coupler design are the bend radius and taper length. By choosing these parameters using intuition from the coupled local mode theory [20–22], power transfer to unwanted modes is reduced. The coupled local mode theory states that the power lost, P_m, to an unwanted mode m is given by

$$P_m(z) \propto 2\left|\frac{\bar{\kappa}}{\overline{\delta\beta}}\right|^2 [1-\cos(\overline{\delta\beta}z)], \quad (1)$$

where $\overline{\delta\beta}$ is the average difference of the propagation constants, $\bar{\kappa}$ is the average value of the coupling coefficient, and z is the direction of propagation along the structure. The coupling coefficient, κ, is given by

$$\kappa_{mn} = \frac{\omega}{4\delta\beta(z)} \int\int \mathbf{e}_m^*(x,y,z)\mathbf{e}_n(x,y,z)\frac{\mathrm{d}}{\mathrm{d}z}\varepsilon(z)\mathrm{d}x\mathrm{d}y, \quad (2)$$

where $\mathbf{e}_m$ is the normalized vector electric field of mode m.

From Eq. (1), it can be seen that power lost to other modes is proportional to the ratio of $\overline{\kappa}$ to $\overline{\delta\beta}$. As $\overline{\delta\beta}$ is in the denominator, power can only be transferred to modes with similar propagation constants, eliminating the problem of modal interference caused by short beat lengths. From Eq. (2), it can be seen that κ is reduced by decreasing $\mathrm{d}\varepsilon(z)/\mathrm{d}z$. Physically, this means any transition must be gradual to minimize the derivative term, so for this coupler, both the bend radius and the taper length should be as large as possible. However, high-speed applications limit the maximum device size, so the desired single-mode operation illustrated in Figs. 1(b) and 1(c) cannot fully be achieved.

A detector length of 12 μm was chosen, providing an adequate trade-off between the coupler length and bandwidth. The fabrication limited the smallest detector width to 1.5 μm, so this detector size was investigated to show the operation of the mode-evolution-based coupler. The bend radius in the coupler was chosen to be 5 μm and spanned the first 2 μm of the detector, placing the bus waveguide 100 nm away from the silicon base of the detector. This bend radius was large enough to not couple power to additional hybrid modes in the Ge-on-Si structure due to the small electric field overlap with modes supported mostly in the germanium. This left 10 μm for the linear taper of the silicon bus waveguide, which is long enough so power is only coupled to a few hybrid modes. The mode-evolution-based coupled photodetectors were compared to butt-coupled detectors of the same size. A three-dimensional (3D) illustration of each configuration is given in Figs. 2(a) and 2(b). Each coupler was simulated using the finite-difference time-domain (FDTD) method with a fundamental TE mode input, as indicated in Figs. 2(a) and 2(b). At the end of the detector, the overlap between the field profile generated by FDTD and each supported mode was calculated. The results are plotted in Fig. 2(c). This simulation indicates that the butt coupler excites modes in the Ge-on-Si structure with vastly different propagation constants, whereas the mode-evolution-based coupler mainly couples power to three similar modes. The beat length (defined as $2\pi/\Delta\beta$) of the two closest modes in the butt-coupled detector is 2.5 μm, and the beat length of the farthest two modes in the mode-evolution-based coupled detector is 11 μm, representing the best case, i.e., the largest and shortest beat length in the butt- and mode-evolution-based coupled detectors, respectively. Thus, the modal interference will be greatly reduced by using the mode-evolution-based coupler to eliminate high-intensity regions that could cause saturation in photocurrent generation. To illustrate this point, the power absorbed in the germanium for each coupling method was simulated using the FDTD method. Cross-sectional views of the absorbed power are shown in Figs. 2(d) and 2(e). It is clear that the butt coupler produces discrete locations of strong power absorption in the first few micrometers of the device due to the beating between modes, whereas the absorption in the mode-evolution-based coupled detector is more distributed throughout the intrinsic region. The more uniform absorption in the germanium will greatly reduce any saturation effects seen at high input powers.

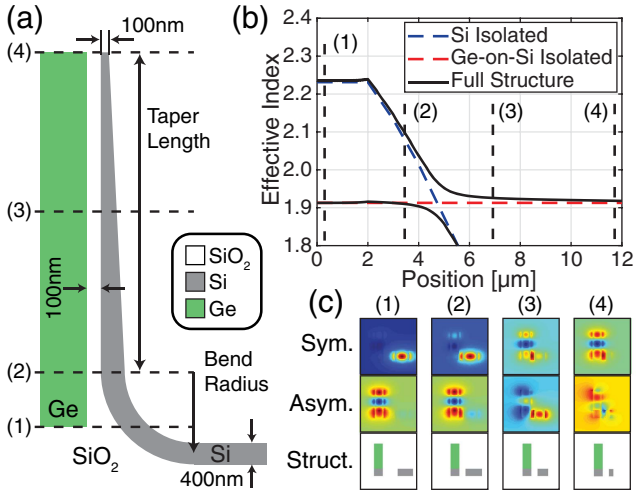

Fig. 1. (a) Not-to-scale diagram of the mode-evolution-based coupler and a simplified Ge-on-Si detector. (b) The effective refractive index of the optical modes as a function of the position at 1550 nm using a 5 μm bend radius and a 10 μm taper length. (c) Cross-sectional views of the TE electric field distribution of symmetric (Sym.) and antisymmetric (Asym.) modes and the structure's refractive index distribution (Struct.).

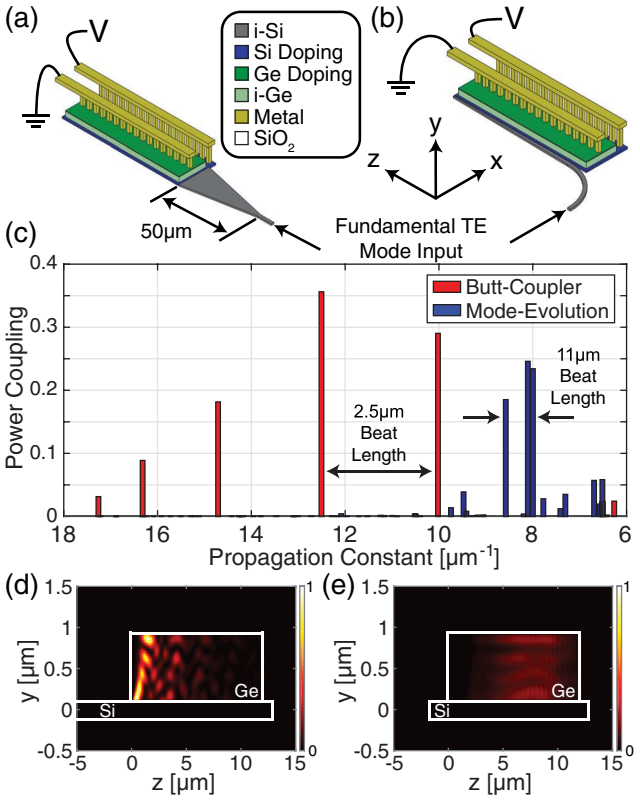

Fig. 2. 3D illustration of the fabricated (a) butt- and (b) mode-evolution-based coupled Ge-on-Si detectors. (c) FDTD simulation of power coupled to each mode for both couplers at 1520 nm. Power absorbed as a function of position for a 1.5 μm × 12 μm photodetector using the (d) butt- and (e) mode-evolution-based coupler at 1520 nm ($k = 0.045$) [23].

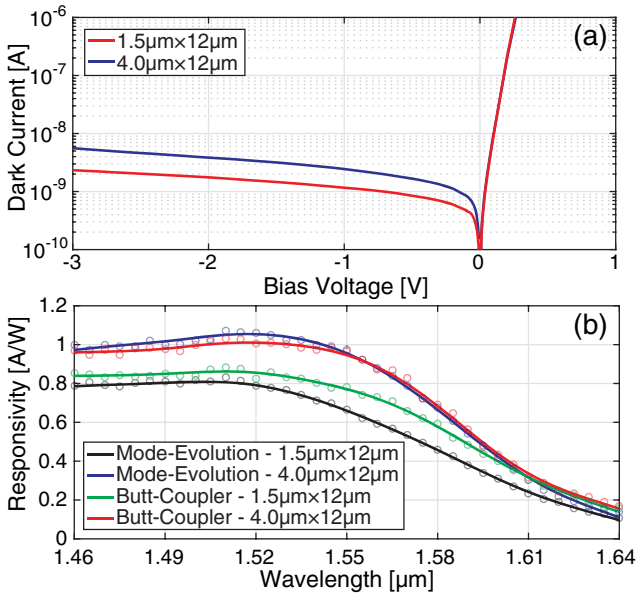

Fig. 3. (a) Measured dark current of 1.5 μm × 12 μm and 4 μm × 12 μm detectors, which is independent of the coupler type. (b) Measured responsivity of 1.5 μm × 12 μm and 4 μm × 12 μm detectors with an 80 μW TE-polarized optical input.

The Ge-on-Si photodetectors were fabricated in a CMOS foundry using 193 nm immersion lithography on a 300 mm SOI wafer with 220 nm silicon height and 2 μm buried oxide. The germanium layer was hetero-epitaxially grown on top of a heavily *p*-doped silicon base with the edges recessed 250 nm inside the silicon. An *n*-type dopant was implanted in the top of the germanium to form a vertical *p-i-n* junction for the detector. Metal layers contacted the *n*-doped germanium and the *p*-doped silicon and were routed to pads for individual testing. Furthermore, each Ge-on-Si detector was fabricated with a butt- and mode-evolution-based coupled input to remove inter-detector variability due to differences in the germanium growth.

The dark current of the Ge-on-Si detectors was measured from −3 to 1 V bias [Fig. 3(a)]. At −1 V bias, the dark current of the 1.5 μm × 12 μm detectors was measured to be 1.16 nA. The responsivity was characterized as a function of the wavelength at a −1 V bias for both the butt- and mode-evolution-based coupling schemes [Fig. 3(b)]. At 1550 nm, the responsivity of the 1.5 μm × 12 μm butt- and mode-evolution-based coupled detectors was measured to be 0.8 and 0.7 A/W, respectively. The difference in responsivity decreases as the detector width increases. At a width of 4 μm, the difference is near zero, and a 1.0 A/W responsivity at 1550 nm was measured.

To show the advantages of the mode-evolution-based coupler, the photocurrent was measured as a function of the input power to a 1.5 μm × 12 μm detector at 1550 nm with a −1 V bias (Fig. 4). The smaller detector size was chosen to increase the power density inside the germanium. The inset in Fig. 4 plots the photocurrent versus the input power on a logarithmic scale to illustrate the large dynamic range spanning roughly 6 orders of magnitude. The full data set shows no saturation effects when using either coupling scheme up to an input of 6 mW. Past 6 mW of input power, a saturation in the photocurrent was observed in the butt-coupled detector, whereas the mode-evolution-based coupled detector continues generating more photocurrent. The small roll-off in photocurrent observed in the mode-evolution-based coupled detector can be attributed to the slightly uneven power absorption [Fig. 2(e)]. At 28 mW of input power, the 1.5 μm × 12 μm detector with the mode-evolution-based coupler produces 15.5 mA of photocurrent, while the same-sized butt-coupled detector generates 9.1 mA, corresponding to an improvement of 70%. Thus, the mode-evolution-based coupling scheme reduces the effect described in [15] and increases the saturation current by more uniformly illuminating the germanium.

The opto-electrical bandwidth of the 1.5 μm × 12 μm Ge-on-Si photodetectors was measured using an optical heterodyne technique where two input lasers at the same power level and polarization for full modulation ($m = 1$) produced a GHz range beat frequency at the photodetector. The device frequency response was then measured in the TE polarization at 1550 nm with −1 V bias to find the 3-dB opto-electrical bandwidth of the detectors. Due to the size of this device, the bandwidth is not RC limited and is instead transient time limited to a calculated value of 40 GHz [7]. The photodetector response versus the beat frequency is plotted in Fig. 5. At a low optical input power of 10 μW in each laser, a transient-time-limited 3-dB bandwidth of 40 GHz was observed in both the butt- and mode-evolution-based coupled detectors. The heterodyne experiment was repeated with a higher input power. With 2 mW of power in each laser, a difference in bandwidth

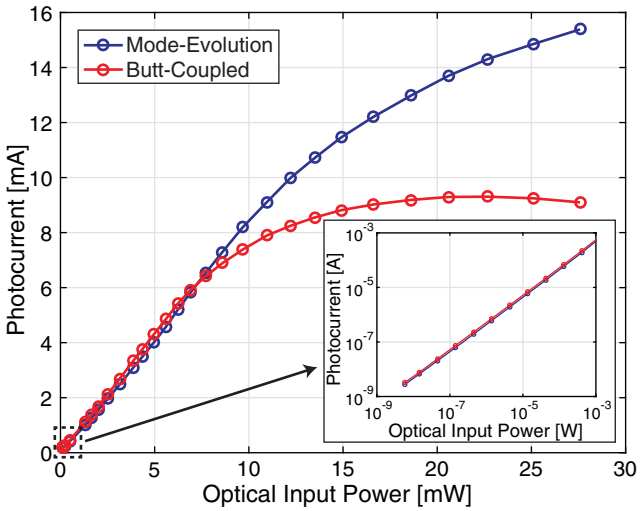

Fig. 4. Measured photocurrent as a function of 1550 nm TE-polarized input power to the 1.5 μm × 12 μm detector for both butt- and mode-evolution-based couplers.

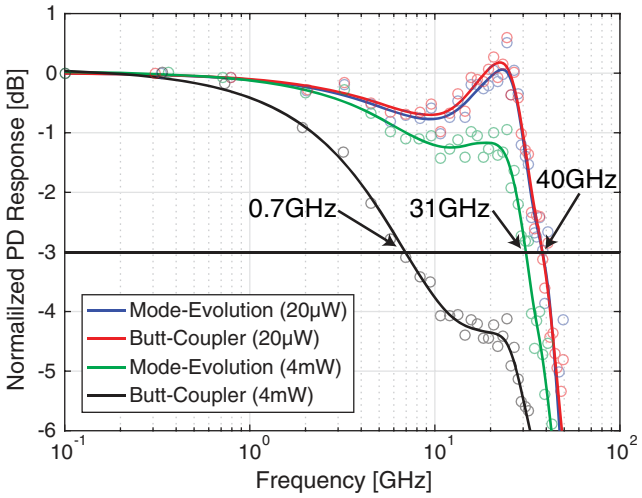

Fig. 5. Measured frequency response of a 1.5 μm × 12 μm detector with each coupler at 20 μW (red and blue curves) and 4 mW total input power (black and green curves).

was observed between the butt- and mode-evolution-based coupled photodetectors. The 3-dB bandwidth of the butt-coupled photodetector decreased to 0.7 GHz, whereas the 3-dB bandwidth of the mode-evolution-based coupled detector only decreased to 31 GHz. This improvement is due to the more uniform absorption of optical power in the germanium, significantly reducing the effects of carrier screening observed in the butt-coupled photodetector [18].

In conclusion, a novel coupling scheme based on mode evolution for Ge-on-Si photodetectors has been demonstrated. The results show that the detector has a low dark current of 1.16 nA, high responsivity at 1550 nm of 1.0 A/W, and a 3-dB opto-electrical bandwidth of 40 GHz. The detector with the mode-evolution-based coupler better maintains these characteristics at high input powers, whereas strong saturation effects are observed in conventional butt-coupled photodetectors. Specifically, the mode-evolution-based coupled detector generates 15.5 mA of photocurrent compared to 9.1 mA in the butt-coupled detector at an input power of 28 mW. At a total illumination power of 4 mW, the mode-evolution-based coupled detector has an opto-electrical bandwidth of 31 GHz compared to 0.7 GHz in the butt-coupled detector. Furthermore, the compact mode-evolution-based coupler takes little additional space and also adds no complexity to the detector, so it can easily replace butt-coupled devices. All these characteristics indicate that this coupling scheme for Ge-on-Si detectors can be useful for many integrated optical systems in the fields of microwave photonics, optical communications, and optical sensing that demand both high-power and high-speed devices.

Funding. Defense Advanced Research Projects Agency (DARPA) (HR0011-12-2-0007); National Science Foundation (NSF) (1122374).

REFERENCES

1. A. Beling, A. S. Cross, M. Piels, J. Peters, Q. Zhou, J. E. Bowers, and J. C. Campbell, Opt. Express **21**, 25901 (2013).
2. X. Wang, N. Duan, H. Chen, and J. Campbell, IEEE Photon. Technol. Lett. **19**, 1272 (2007).
3. H.-C. Luan, D. R. Lim, K. K. Lee, K. M. Chen, J. G. Sandland, K. Wada, and L. C. Kimerling, Appl. Phys. Lett. **75**, 2909 (1999).
4. J. Michel, J. Liu, and L. C. Kimerling, Nat. Photonics **4**, 527 (2010).
5. T. Yin, R. Cohen, M. M. Morse, G. Sarid, Y. Chetrit, D. Rubin, and M. J. Paniccia, Opt. Express **15**, 13965 (2007).
6. L. Vivien, J. Osmond, J.-M. Fédéli, D. Marris-Morini, P. Crozat, J.-F. Damlencourt, E. Cassan, Y. Lecunff, and S. Laval, Opt. Express **17**, 6252 (2009).
7. D. Feng, S. Liao, P. Dong, N.-N. Feng, H. Liang, D. Zheng, C.-C. Kung, J. Fong, R. Shafiiha, J. Cunningham, A. V. Krishnamoorthy, and M. Asghari, Appl. Phys. Lett. **95**, 261105 (2009).
8. L. Vivien, A. Polzer, D. Marris-Morini, J. Osmond, J. M. Hartmann, P. Crozat, E. Cassan, C. Kopp, H. Zimmermann, and J. M. Fédéli, Opt. Express **20**, 1096 (2012).
9. C. T. DeRose, D. C. Trotter, W. A. Zortman, A. L. Starbuck, M. Fisher, M. R. Watts, and P. S. Davids, Opt. Express **19**, 24897 (2011).
10. H. Chen, P. Verheyen, P. De Heyn, G. Lepage, J. De Coster, S. Balakrishnan, P. Absil, W. Yao, L. Shen, G. Roelkens, and J. Van Campenhout, Opt. Express **24**, 4622 (2016).
11. Y. Zhang, S. Yang, Y. Yang, M. Gould, N. Ophir, A. E.-J. Lim, G.-Q. Lo, P. Magill, K. Bergman, T. Baehr-Jones, and M. Hochberg, Opt. Express **22**, 11367 (2014).
12. R. Going, T. J. Seok, J. Loo, K. Hsu, and M. C. Wu, Opt. Express **23**, 11975 (2015).
13. S. Liao, N.-N. Feng, D. Feng, P. Dong, R. Shafiiha, C.-C. Kung, H. Liang, W. Qian, Y. Liu, J. Fong, J. E. Cunningham, Y. Luo, and M. Asghari, Opt. Express **19**, 10967 (2011).
14. G. Li, Y. Luo, X. Zheng, G. Masini, A. Mekis, S. Sahni, H. Thacker, J. Yao, I. Shubin, K. Raj, J. E. Cunningham, and A. V. Krishnamoorthy, Opt. Express **20**, 26345 (2012).
15. A. R. Schaefer, E. F. Zalewski, and J. Geist, Appl. Opt. **22**, 1232 (1983).
16. K. J. Williams and R. D. Esman, IEEE Photonics Technol. Lett. **10**, 1015 (1998).
17. K. Williams and R. Esman, Electron. Lett. **28**, 731 (1992).
18. K. S. Giboney, M. J. Rodwell, and J. E. Bowers, IEEE J. Sel. Topics Quantum Electron. **2**, 622 (1996).
19. C.-M. Chang, J. H. Sinsky, P. Dong, G. de Valicourt, and Y.-K. Chen, Opt. Express **23**, 22857 (2015).
20. M. R. Watts and H. A. Haus, Opt. Lett. **30**, 138 (2005).
21. M. R. Watts, H. A. Haus, and E. P. Ippen, Opt. Lett. **30**, 967 (2005).
22. A. W. Snyder and J. Love, *Optical Waveguide Theory* (Chapman & Hall, 1983).
23. E. D. Palik, *Handbook of Optical Constants of Solids* (Academic Press, 1997).